

# USER GUIDE TO THE GIADA MEASUREMENTS IN THE PSA PLANETARY SCIENCE ARCHIVE (PSA)

prepared by V. Della Corte

User Guide to the GIADA Measurements in the PSA Planetary Science Archive (PSA).....	1
Instrument Overview.....	3
Dust flux measurement for “direct” and “reflected” grains.....	5
Analysis of the dust velocity distribution .....	5
Correlation of dust changes with nucleus evolution and emission anisotropy.....	6
Operational modes and science data produced.....	7
Mode transition table.....	7
Safe Mode.....	8
Normal Mode.....	8
Flux Mode .....	8
Science data produced linked to science goals .....	9
Typical scientific analysis .....	9
Dust mass production and Dust to Gas ratio evaluation.....	9
Description of the data present in the PSA linked to the scientific analysis .....	9
Recommended software .....	10
Data processing .....	10
Level 3 elaboration .....	10
Particle flux and mass evaluation .....	11
Maps evaluation .....	11
map of Particle Speed and maps of Speed range evaluation .....	11
Nucleus areas dust production.....	12
Example dataset time period which can be used to learn processing steps.....	14
List of caveats - problems with data contents, format.....	15
List of science papers where further information can be found .....	15

## Instrument Overview

GIADA is a single box shaped instrument, 230 mm x 270 mm x 250 mm in cruising mode, when the cover is closed, and 230 mm x 322 mm x 250 mm in operational mode (box only, without feet). Refer to Figure 1 for a 3-D view of the experiment in its open configuration. Three modules compose the instrument: GIADA 1 measures momentum, scalar velocity and mass of single grains entering the instrument by the Grain Detection System (GDS) and the Impact Sensor (IS); it also hosts the cover that protects this module and GIADA 3 during off phases. The GIADA 2 module contains the Main Electronics (ME); it controls the acquisition of data from the sensors and the operation of the other subsystems. It also provides the power supply for the whole experiment. The GIADA 3 module measures the cumulative dust flux and fluence from different directions by 5 microbalances (MBS's). One points towards the nucleus, while the other four cover the widest possible solid angle. The MLI that thermally insulates the experiment from the environment and the sun covers all the external surfaces of the experiment. The upper part of the GIADA 1 box houses, together with GDS and IS, the locking mechanism and the protective cover with associated PEs. The bottom part of the box contains GIADA 2, while the top plate supports the five MBS's with associated PE (GIADA 3).

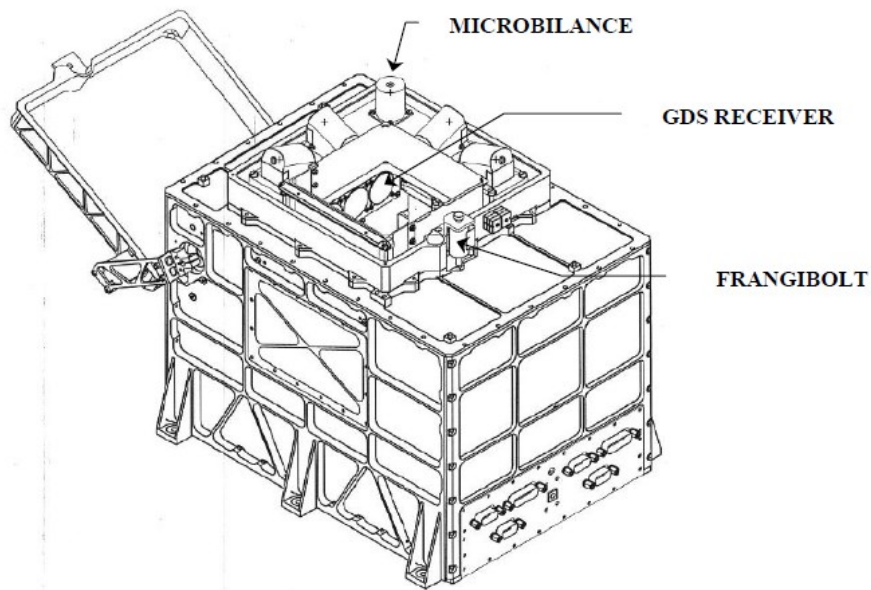


Figure 1 External view of GIADA with cover open

A functional scheme of GIADA, with measurements performed by each detection element, is reported in Figure 2, while a sketch of the GIADA internal configuration is shown in Figure 3, where the GDS and IS placed in cascade can be seen.

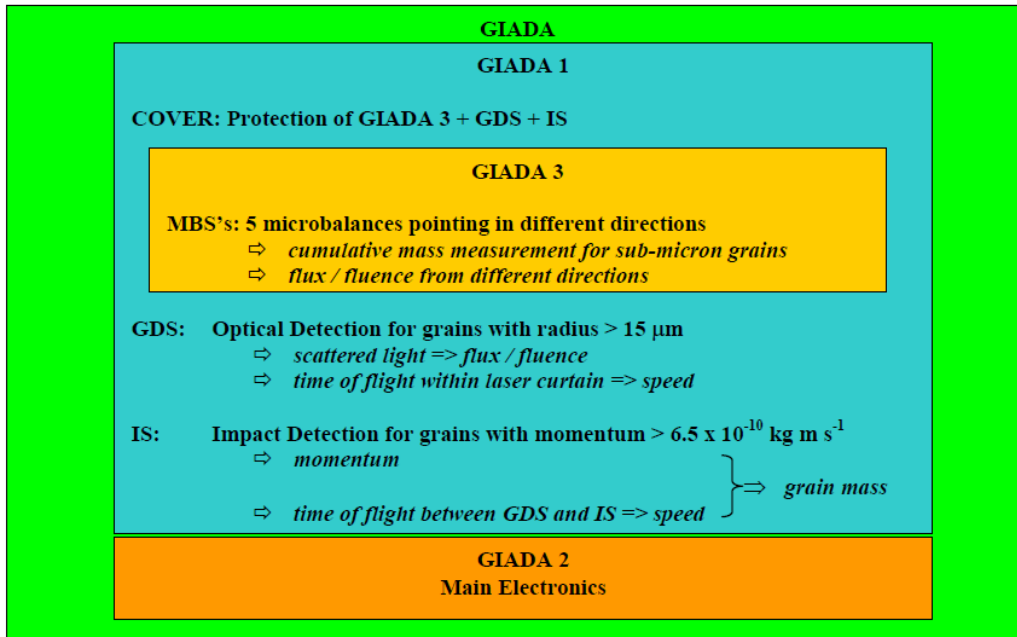


Figure 2 Block diagram of GIADA and performed measurements

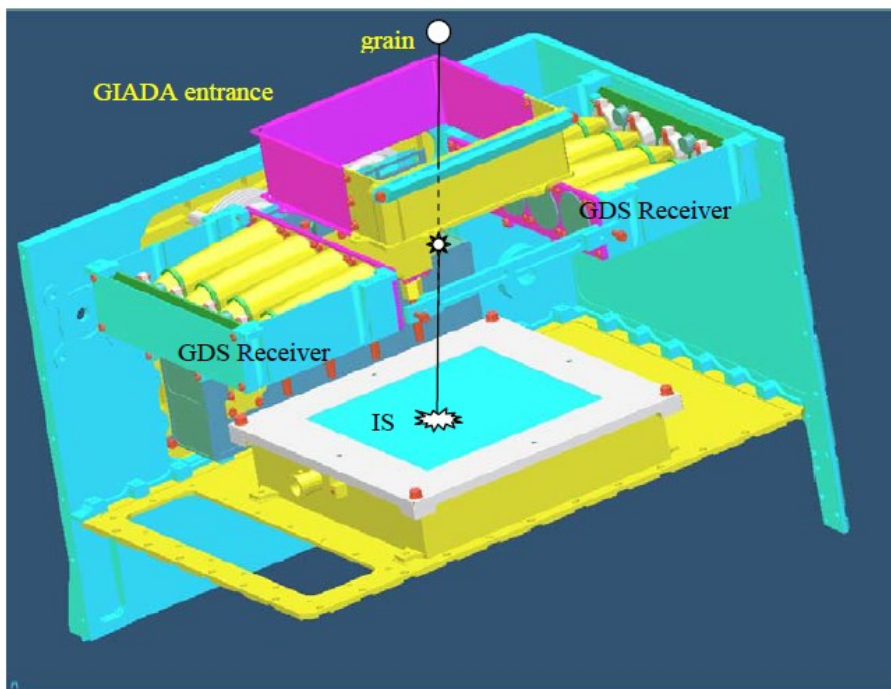


Figure 3 Sketch of the internal configuration of GIADA, where entrance, GDS receiver

The Grain Detection System is formed by an illuminator and two receiver groups. In the illuminator, four laser diodes with their fore optics are used to form a thin (3 mm) light curtain (100 cm<sup>2</sup>). For each grain passing through it, the scattered/reflected light is detected by the two receiver groups: 2 series of four detectors (photodiodes) placed at 90 deg (left and right sides of the light curtain) with respect to the sources. In front of each photodiode a Winston cone is placed to achieve a uniform sensitivity in the detection area. The Impact Sensor is a thin (0.5 mm) aluminium square diaphragm (sensitive area 100 cm<sup>2</sup>) equipped with five piezoelectric sensors, placed below the corners and its centre. When a particle impacts the sensing plate, flexural waves are generated on the plate, and are detected by the piezoelectric transducers. The maximum displacement of these systems is directly

proportional to the impulse imparted, and the displacement of the crystal produces a proportional potential. Through calibration, a known impulse may be equated with a specific charge produced on the electrodes of the PZT crystals. The detected signal is proportional to the momentum of the incident grain through the factor  $(1+e)$ , with  $e$  = coefficient of restitution. When a particle enters GIADA 1, the GDS gives a first estimate of the grain speed and starts a time counter that is stopped when the IS detects the grain impact and the momentum is measured. In this way for each entering particle, speed, time-of-flight, momentum and, therefore, mass are measured. Each Micro-balance consists in two (sensor and reference) quartz crystals oscillating at a frequency of about 15 MHz, with a shift of some kHz. The measured physical quantity is the beat frequency between the two crystals. The resonance frequency of the sensor quartz oscillator, exposed to the dust environment, changes due to the variation of its mass, as a result of material accretion, while the reference crystal is not exposed to the dust flux. Thus, the output signal is proportional to the mass deposited on the sensor and dust flux and fluence are measured in time. The use of a reference crystal ensures extremely small dependence on temperature and power supply fluctuations and, thus, high sensitivity. The primary scientific objectives of GIADA (Grain Impact Analyser and Dust Accumulator) are described in the follows.

### DUST FLUX MEASUREMENT FOR “DIRECT” AND “REFLECTED” PARTICLES

Two populations of cometary particles do exist: “direct” (coming directly from the nucleus) and “reflected” particles (coming from the sun direction, under the action of the solar radiation pressure). The two populations have extremely different dynamic evolution in the coma and ejection times from the nucleus. In the case of ROSETTA, “direct” and “reflected” particles can be collected simultaneously. The relative amount will depend on the probe position along its orbit. GIADA monitored particle fluxes coming from different directions and allowed for the first time to discriminate the two dust populations. This task is fundamental to determine the original dust size distribution. In turn, this determination is mandatory to define the dust mass loss rate.

### ANALYSIS OF THE DUST VELOCITY DISTRIBUTION

The dust ejection velocity depends both on the particle size and on time. Moreover, particles with a given size have a wide dust velocity distribution. GIADA measured scalar velocity and momentum for particles coming from the nucleus direction giving mass and impact velocity of each analysed “direct” particle. From this information it was possible to derive particle mass and ejection terminal velocity from the nucleus surface. For the first time we obtained:

- a) the size dependence of the dust ejection velocity;
- b) the relation between most probable dust velocity and dust mass;
- c) the velocity distribution for each dust mass;
- d) the link between velocity dispersion and dust mass.

### STUDY OF DUST EVOLUTION IN THE COMA

Once ejected from the nucleus, particles may change their physical properties due to several processes (e.g. fragmentation). These modifications may alter the particle size distribution. The size distribution of particles collected by GIADA in the nucleus direction should not be affected by the dust velocity dispersion. Thus, changes in the dust distribution at different nucleus distances can be linked directly to actual variations in the dust size

distribution and correlation can be found with dust fragmentation and/or with emission from active areas on the nucleus.

## CORRELATION OF DUST CHANGES WITH NUCLEUS EVOLUTION AND EMISSION ANISOTROPY

The dust environment characteristics depend on the comet-sun distance and on the time evolution of the nucleus. The continuous monitoring by GIADA of dust flux and dynamic properties offers the opportunity to characterise the time evolution of the dust environment as a function of heliocentric distance. Nucleus imaging allows to link observed changes to the nucleus evolution and to its spin state.

## DETERMINATION OF DUST TO GAS RATIO

One of the crucial parameters characterising the comet nucleus is the dust to gas ratio. The dust flux monitoring by GIADA is absolutely needed to estimate the dust to gas ratio. This is possible in combination with results of other experiments (e.g. the mass spectrometer).

## Operational modes and science data produced

GIADA has been operated for scientific data acquisition starting from the approach phase to the comet and until the end of the ROSETTA mission. This means that during the long cruise phase GIADA was generally switched off but for limited periods of time, that are needed to check periodically the health status of the experiment and to test the functionality of its sub-systems, was operative and collected data that allowed us to characterize the instrument noise behaviour. The science operation of GIADA started since the mapping phase and continued for the rest of the mission.

### MODE TRANSITION TABLE

GIADA has four operative modes, as reported in Table 1., where sequences to access the different modes are also listed. Allowed transitions are shown Figure 4

Table 1 GIADA operative modes and transition sequences

Mode Name	Active subsystems	Measured quantities
Safe Mode	ME	None
Normal Mode	ME, GDS, 5 MBSs, IS  Note: actual number of sensors used depends on the Context File content	Dust flux and fluence Grain Scattering properties Momentum of single grains Velocity of grains Mass of single grains
Flux Mode	ME, 5 MBSs	Dust flux and fluence
Cover Mode	ME, Cover or Frangibolt Electronics	N/A

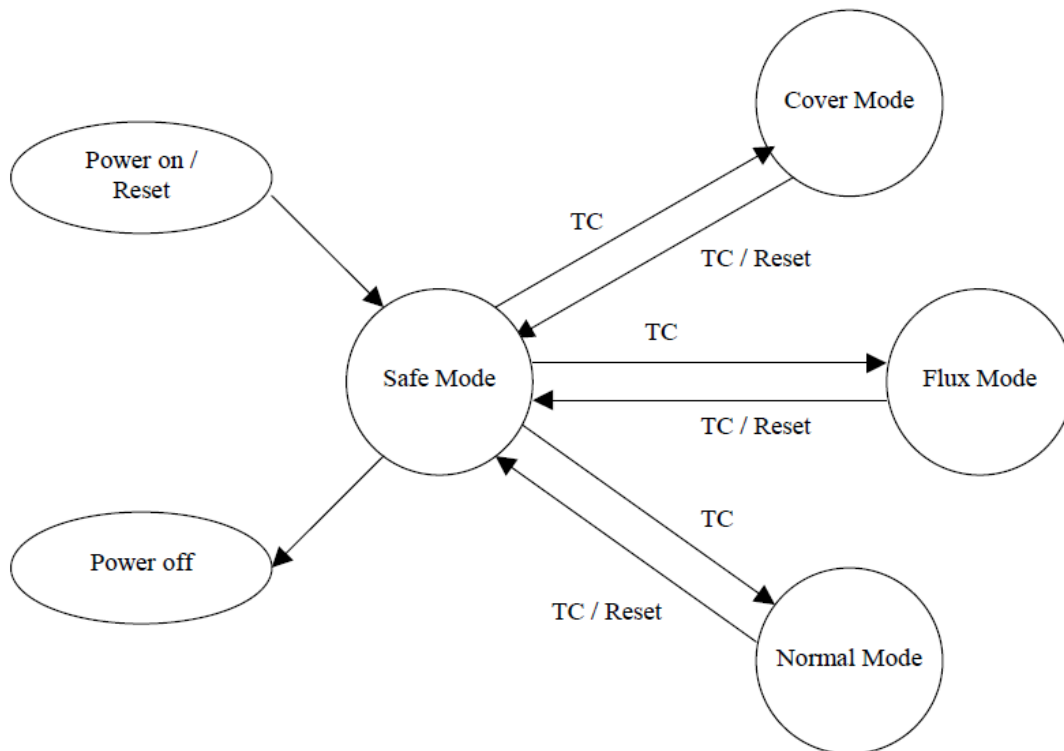


Figure 4 GIADA Operative Modes

## SAFE MODE

This mode is entered, by default, after either power-on or reset. Only the Main Electronics is running; the on-board S/W runs from PROM. In this mode no scientific measurements are taken, and the instrument waits for a TC to begin normal operations. The only data that are collected and sent on the OBDH bus are the HK information, unless the relative TC has stopped their delivery. This mode allows time synchronisation, TC execution and memory manipulations (patches and dumps). All the sub-systems are initialised in power-off condition after software boot. After a power-on/reset, the on-board software is first copied from PROM to RAM, and then a jump to the first valid code address in PROM is performed. The H/W and S/W initialisation activities, including a check of the validity of the NVRAM contents, are performed; the instrument is then ready to receive the commands. GIADA goes to Safe mode immediately after power and GIADA was able to accept and execute all the relevant commands, even the ones that imply an operative mode change.

## NORMAL MODE

This is the operative mode of GIADA during nominal S/C and instrument operational conditions where every subsystem is running. The onboard S/W runs in RAM. Only after receiving a proper mode transition command ('Go to Normal'), this operative mode is entered. After entering Normal mode, depending on the actual Configuration Table status, the sub-systems are sequentially switched on but the GDS Laser Illuminator, which requires a sequence of two telecommands, issued by a proper OBCP procedure. This OBCP procedure is triggered by GIADA S/W via an On-board Action Anomalous Event report that is sent every time the GDS is switched on. No science TM packets issued from GIADA until the corresponding TC has enabled the science packet generation. At this point GIADA performed the scientific acquisitions (periodically, in the case of the MBS which are read every 300 s, and event driven, for the IS and GDS subsystems).

Other periodic activities that run in Normal Mode are:

- HK data acquisitions every 40 s or 10s;
- Subsystems temperature monitoring every 60 s;
- GDS, IS and MBS self-calibration (generation of specific scientific TM) every hour.

### *IS internal calibration behaviour*

The IS calibration stimulus is a voltage pulse of a pre-defined level that is applied to the stimuli piezo. The calibration is periodic or triggered by ground TC. The voltage level and number of stimuli depend on parameters in the Configuration Table (when autonomous) or on TC parameters. The stimuli piezo provides a mechanical stimulus to the IS sensor plate which is detected by the five detection piezoelectric sensors. Two mechanical stimuli occur when the voltage rises to the pre-defined level and when it falls to 0V. Between the two edges, a time delay of about 1 s is foreseen to catch the detections. Two IS detections correspond to one voltage pulse. The IS calibration (autonomous and by ground TC) is used to observe the behaviour of the IS sensor in time and in different environment conditions (i.e. different steady-state temperatures).

## FLUX MODE

Only the five microbalance (MBS) sensors and the main electronics could, then, be active. The switching to Flux mode happens by means of proper TC, when GIADA is in Safe mode. The HK acquisition and transmission are also enabled in this mode, as well as the monitoring of the thermistor placed on the IS plate,

## Science data produced linked to science goals

### Typical scientific analysis

#### DUST MASS PRODUCTION AND DUST TO GAS RATIO EVALUATION

The dust to gas ratio measured by the team and reported in [1] [5] [8] was measured combining the dust production rates measured by GIADA with the measured dust emission measured by the OSIRIS images and by the gas production rates published by the ROSINA team. The analysis process used is described in [8] and reported in the following.

To retrieve a meaningful dust/gas ratio, we assume the same hemispherical dust ejection. If both gases and dust are ejected within a smaller solid angle, we will overestimate both the gas and the dust mass loss rates, but we will still obtain the correct dust/gas mass ratio. From the GDS+IS events with measured momentum and speed from which we can calculate the particle mass ( $m$ ) directly. We compute the derived mass loss rate per particle at the nucleus :  $Q_m = 2\pi m R^2 (A \Delta t)^{-1}$  where  $\Delta t$  is the collection time,  $R$  is the distance of the spacecraft from the nucleus center of mass, and  $A$  is the effective IS collecting area. Because the spacecraft radial velocity is much smaller than the dust velocity, the conversion from observed impacts to dust loss rate at the nucleus does not depend on the dust velocity. For the IS only detected particles the particle speed ( $v$ ) is therefore derived from a model applied to ground-based observations of 67P or using empirical equation retrieved by the GIADA data. To complement the GIADA data and to estimate the largest dust mass ejected from 67P, we consider the detections of single particles by the OSIRIS narrow-angle camera (NAC). We compute the velocity of the outflowing particles assuming that the particle motion is strictly radial from the nucleus. For the OSIRIS detections, the dust loss rate was extracted from the dust space density  $\rho$  at the spacecraft, which was computed on coma volumes defined by the distance  $D$  from the spacecraft to the faintest (just above the detection limit) grain in each mass bin (i.e., the coma volume surveyed by the OSIRIS-NAC).  $N$  is the number of detections (for the OSIRIS data,  $N$  was divided by the number of images providing independent detections),  $v$  is the mean dust radial velocity (thus canceling out transverse speed effects), and  $Q_n$  is the number loss rate for hemispherical dust ejection

$$Q_n = 2\pi r v R^2$$

For the GIADA detections, the dust mass loss rate per mass bin ( $Q_m$ ) is the sum of all  $Q_n$  values.

### Description of the data present in the PSA linked to the scientific analysis

The data present in the dataset level 3 are directly linked to the scientific analysis as described in the Data processing paragraph. In particular, the data contained in the PHYSDATA table in the level 3 dataset, are self-consistent and can be directly used to retrieve the main scientific results obtained by GIADA.

## Recommended software

No dedicated software is foreseen for the GIADA data analysis, any SW package able to retrieve data from csv ASCII data tables and to perform statistical analyses can be used to elaborate the GIADA measurements.

## Data processing

### LEVEL 3 ELABORATION

In the LEVEL 3 GIADA dataset the data collected by the IS subsystem and the GDS+IS subsystems are fully calibrated. The physical quantities obtained by the calibration chain on the raw data obtained from the telemetry are reported in the PHYSDATA table contained in each GIADA dataset level 3 produced for the scientific phase of the ROSETTA mission.

In the LEVEL 3 dataset no calibrated data is provided for the detection obtained only by the GDS subsystem. The data collected by the GDS are only reported at the LEVEL 2 elaboration. The calibration of this data is strongly linked to the actual particle composition and to their optical properties. To retrieve the particles cross section from the measurements performed by GIADA several assumptions are needed to select the right calibration curves obtained by means of cometary particle analogues during the calibration sessions in the laboratory.

For the calibration of the data to retrieve Particles cross-sections, interaction with the GIADA team are mandatory. In any case to analyse the level 2 data contained in the delivered dataset some precautions and prescriptions need to be followed considering that:

- 1) The GDS detection is driven by a threshold mechanism
- 2) The subsystem is extremely sensitive to the straylight
- 3) The Sun illumination angle is a strong possible source of false detections.

During the cruise phase several payload check-outs have been performed. During the checkout all the subsystems have been tested and used for representative measurement time. The analysis of the data collected during these tests allowed us to characterize the behaviour of the measurement subsystems.

Considering that each GDS detection is composed of two parameters: an amplitude and a duration, the most important instrumental effect for the GDS is the randomly appearance of false detections with short duration. The subsystem identifies as a real detection only the particles that have travel time in the laser curtain longer than 30 microseconds (this is a HW limit).

During the cruise phase several false detections of variable amplitude but characterized by short duration have been registered. This behaviour forced us to select as scientific detections only the detections with duration greater of a certain value.

The analysis of the data collected during the cruise phase forced us to change this value to travel time greater than 60 microseconds. This selection was not applied neither by the instrument in the telemetries neither to the level 2 data in the dataset, it has to be applied when the data are used.

## PARTICLE FLUX AND MASS EVALUATION

GIADA characterises individual dust particles by means of two independent sensors. At the instrument entrance the particle crosses a laser curtain, and is detected by photoelectric sensors (GDS, Grain Detection System) registering a signal (proportional to the particle cross-section times the albedo) and the laser curtain crossing time. Then the particle hits the Impact Sensor (IS, with the same GDS cross section,  $A = 10^{-2} \text{ m}^2$ ), which registers individual particle impact momentum and its travel time from GDS to IS. The combination of GDS and IS measurements (GDS+IS particles) provides the particle mass and velocity. In addition, the combined measurements constrain the particle bulk density by means of calibration curves derived on ground using cometary analogues. If the particle is too small to be detected by the GDS system, it may be detected by the IS sensor only (IS particles): in this case the particle momentum is converted to the mass assuming the mean value of the velocities of the GDS+IS particles in the same momentum bin, or assuming the velocities predicted by tail models [10] if  $N_{\text{gds+is}} = 0$  in that mass bin. The spacecraft velocities listed are always much lower than the dust velocities measured by GIADA. In this condition, in the sun-facing coma (assumed to have uniform space density), the dust flux from the nucleus surface corresponds to the dust flux at nadir-pointing GIADA scaled by the factor  $2\pi R^2/A$ . The dust number loss rate at the nucleus surface per GIADA detection is  $Q_n = 2\pi R^2 [A \Delta t]^{-1}$ , where  $\Delta t$  is the total dust collection time. The mass loss rates  $Q_m$  and the mean dust velocities are retrieved with the same procedure considering the number of particles in each mass bin measured by GIADA.

## MAPS EVALUATION

To reconstruct the coma dust Maps we reported GIADA detections in the comet Centred Solar Orbital (CSO) reference frame defined as:

- X axis points from the comet to the Sun.
- Y axis is the component of the inertially referenced Sun velocity relative to the comet and orthogonal to the X axis.
- Z axis is X cross Y, completing the right-handed reference frame.

The CSO reference frame seems the more appropriate to describe the coma dust distribution, highlighting the direct link between the nucleus illumination condition and the coma dust spatial density. In order to obtain maps of dust density at a normalised distance, we proceeded as follows: we applied an additional coordinate transformation from Cartesian to spherical CSO coordinates; we weighted each detection with the time spent by Rosetta in the specific illumination condition, i.e. for the specific orbit phase angle; we weighted each detection by the square of the ratio between the detection distance and the minimum 67P – Rosetta distance in the considered period. we computed a 2D dust detections histogram as a function of spherical CSO coordinates.

## MAP OF PARTICLE SPEED AND MAPS OF SPEED RANGE EVALUATION

GIADA measured the speed of the particles directly by means of the two subsystems GDS+IS. For several other particles GIADA was able to measure the momentum of the particles by means of the IS subsystem. As reported in [3] empirical equations linking the dust mass and the dust speed were retrieved from the analysis of the data collected on particles measured both by GDS and IS. From the analysis the relation  $v = Am^\gamma$ , where  $v$  is the particle speed,  $m$  is the particle mass,  $A$  and  $\gamma$ , are parameters depending on the heliocentric distance and on the

phase angle, has been obtained. We applied this empirical relation together with the real measurement of the IS, that provides the Momentum of each particle to the entire GIADA dataset, in order to retrieve the velocity of dust particles detected by the IS only.

With the obtained values of the speed we constructed a spatial 2d histogram of the speed measured. For each spatial bin we evaluated the average and the standard deviation. Considering the same reference frame used for the Flux and Mass map distribution we constructed 2 maps of the speeds in the 67P coma. In the first map we reported the average values calculated, representing the mean speed of dust particles in the considered area, in the second map we reported the  $3\sigma$  ( $3 \times$  the calculated standard deviation) representing the range of the speed measured in the considered area.

## NUCLEUS AREAS DUST PRODUCTION

In this case we used a standard format for the map considering a reference frame attached to the 67P/C\_G body. We consider a body-fixed reference frame and a “simple cylindrical” projection. In the maps are reported the values of dust particles emitted per unit area expressed as  $\text{deg}^2$  considering the Lat-Lon coordinates in the body fixed reference frame. An indicator of dust cometary activity can be defined as the number of particles ejected by a certain region/area. We developed an algorithm, based on particle velocity measured by GIADA, to reconstruct the motion of each dust particle detected in the coma and tracing it back to the surface, taking into account the spacecraft distance from the nucleus and the comet rotation.

We performed a specific analysis of dust showers [7] applying the following procedure:

- a. Definition of the shower: a shower is defined by all particles detected by GDS at a temporal distance lower than one second with respect to the previous detection;
- b. Retrieval of the parent particle’s velocity.

Case 1: The shower includes a particle detected by GDS+IS, thus its velocity is assumed as the parent particle’s velocity.

Case 2. The shower consists of GDS-only detections, thus we proceed as follow:

- We remove detections measuring speeds  $< 0.3$  m/s, corresponding to fragments disturbed by the spacecraft potential [7];
- We remove detections measuring speeds  $> 45$  m/s, corresponding to poorly reliable measurement because of GDS system behaviour.
- We build a velocity histogram with bins of 5 m/s and we assume the median velocity in the most populated bin, representative of the entire shower velocity, as the parent particle’s velocity.

Even if in the shower velocity distributions speeds  $> 15$  m/s could be less reliable [7], we include these detections in our procedure as they are not statistically significant, and their inclusion does not change our conclusions.

In order to reconstruct the particle’s motion back to the nucleus and identify the geomorphological region from which each particle detected by GIADA was ejected, we made the following assumptions on the particle motion:

1. is radial from the nucleus to GIADA. This assumption is partially corroborated by the results obtained by [3]
2. is uniformly accelerated up to a distance of 11 km from the surface and then rectilinear uniform. This assumption is based on coma dust models [2].

From these assumptions and by means of the algorithm:

- We calculated the particle time of flight from the nucleus surface to GIADA and quantified the comet rotation relative to this time interval.
- By combining time of flight and comet rotation, we identified the geomorphological region from which each particle was ejected.
- We performed a correlation analysis by means of the Pearson coefficient, before and after the application of the traceback algorithm, between: 1) the number of fluffy fragments and compact particles coming from each region; 2) the number of parent and compact particles coming from each region. Because the number of fluffy particles depend on the fragmentation process, the number of parents is more indicative of the actual ejected fluffy particles from each region.

## MAPS PRODUCTION VALIDATION

The procedure to obtain the maps for speed and particle fluxes (mass and number of particles) need to rescale the measurements obtained by GIADA to a single distance from the nucleus. The process of rescaling the measurements to a single distance from the nucleus apply as a scale factor the factor  $(R_{\min}/R)^2$  where  $R$  is the distance of the detection from the nucleus and  $R_{\min}$  is the smaller detection distance for the period considered for the map.

In order to validate, by a numerical 3D+T model, this scaling process we performed several “ab-initio” simulations for each of the maps period. We carried out the simulation retrieving the values of the parameters reported in the maps at different distances (comparable with the distances of the real measurements of GIADA). The simulation have been carried out using particle sizes in the range of the particles detectable by GIADA. The output of the simulation are synthetic maps of the dust properties (mass distribution, speed, particle spatial density) at different distances from the nucleus.

In order to check the  $(R_{\min}/R)^2$  scaling factor we compared the maps at different distances. Using this approach, we selected the right distance (different for different phase of the mission) at which the scaling can be applied.

One example of the maps obtained are reported in Figure 5 and Figure 6. We applied the scaling to the synthetic maps and validate the scaling factor if the error between the rescaled map and the independent solution is less than 15%.

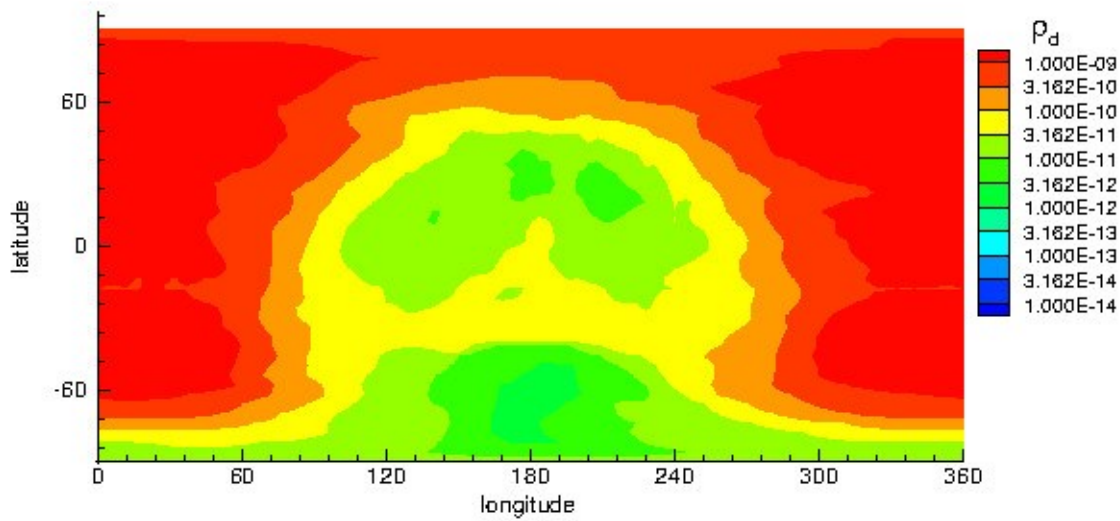


Figure 5 Dust (size 100 microns) spatial distribution at 15 km during the flyby period

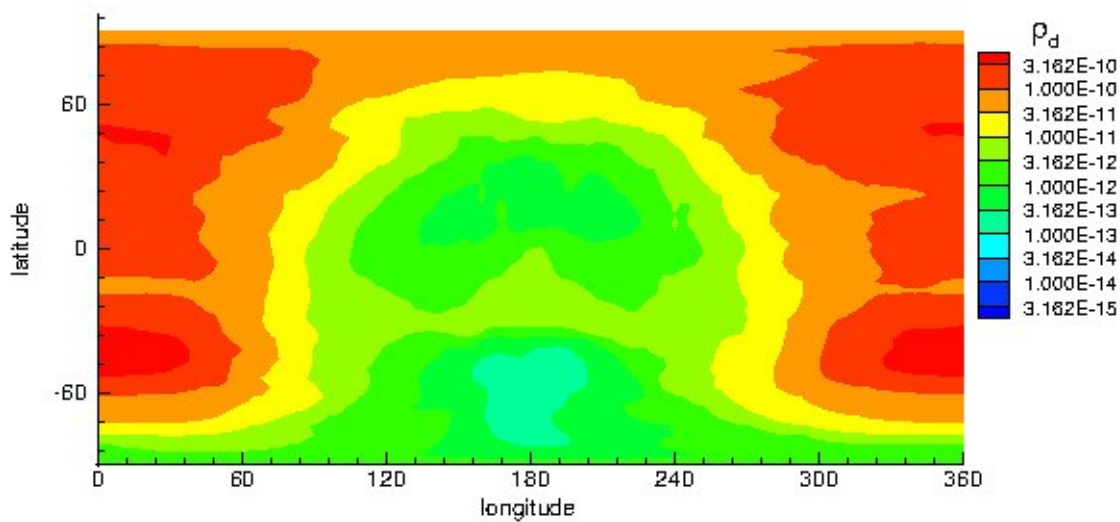


Figure 6 Dust (size 100 microns) spatial distribution at 50 km during the flyby period

## Example dataset time period which can be used to learn processing steps

In each Level 3 Dataset delivered to the PDS small Body node or to the PSA is present an ASCII table with all the detections calibrated. Using this table, it is possible to process the data with the same procedures applied to obtain the level 5 maps reported in the high-level dataset. The information reported in the table needs to be integrated with detailed geometrical information: relative position between Rosetta Spacecraft and the comet nucleus and

the phase angle of the Rosetta orbit. These values can be retrieved by means of the NAIF spice toolkit and the SPICE kernels of the Rosetta mission available on the PSA data archive.

The data collected during the period February 2015 March 2015 are the more complete and can be retrieved by the PHYSDATA table of the ESCORT1 and ESCORT2 datasets of the GIADA instrument.

## List of caveats - problems with data contents, format

The maps are obtained in some case using data from a long period and reporting all this data in a single map, this approach can be considered acceptable when the observation condition remain similar and when the Comet heliocentric distance has small difference during the period. For the Post Perihelion maps these prerequisites is only partially valid. In fact, during this period the Rosetta S/C performed trajectories with largely different orbital parameters, we applied in any case the processing described in the previous paragraph because the large part of the detections occurred in similar observation conditions.

The maps of speed are obtained retrieving not only the speed of the particles detected by both GDS and IS but also the speed of the particles detected only by the IS. These values are obtained applying the process described in [3]. The values of the speed obtained by this process are affected by error bars larger than the speed values obtained by the direct measures performed by the combination of the GDS-IS measurements. When speeds values are retrieved by the maps it is necessary to take into account this issue: while the error on the speed measured by the GDS-IS detection have errors, in all the cases, smaller than the 25% of the measurements, in the case of the speed retrieved by the IS only measurements the error on the measured value is always in the order of the 50% .

## List of science papers where further information can be found

- [1] Title:** The dust-to-ices ratio in comets and Kuiper belt objects  
**Authors:** [Fulle, M.](#); [Della Corte, V.](#); [Rotundi, A.](#); [Green, S. F.](#); [Accolla, M.](#); [Colangeli, L.](#); [Ferrari, M.](#); [Ivanovski, S.](#); [Sordini, R.](#); [Zakharov, V.](#)  
**Publication:** Monthly Notices of the Royal Astronomical Society, Volume 469, Issue Suppl\_2, p.S45-S49 ([MNRAS Homepage](#))  
**Publication Date:** 07/2017
- [2] Title:** Dynamics of aspherical dust grains in a cometary atmosphere: I. axially symmetric grains in a spherically symmetric atmosphere  
**Authors:** [Ivanovski, S. L.](#); [Zakharov, V. V.](#); [Della Corte, V.](#); [Crifo, J.-F.](#); [Rotundi, A.](#); [Fulle, M.](#)  
**Publication:** Icarus, Volume 282, p. 333-350. ([Icarus Homepage](#))  
**Publication Date:** 01/2017
- [3] Title:** 67P/C-G inner coma dust properties from 2.2 au inbound to 2.0 au outbound to the Sun  
**Authors:** [Della Corte, V.](#); [Rotundi, A.](#); [Fulle, M.](#); [Ivanovski, S.](#); [Green, S. F.](#); [Rietmeijer, F. J. M.](#); [Colangeli, L.](#); [Palumbo, P.](#); [Sordini, R.](#); [Ferrari, M.](#);

[Accolla, M.](#); [Zakharov, V.](#); [Mazzotta Epifani, E.](#); [Weissman, P.](#); [Gruen, E.](#); [Lopez-Moreno, J. J.](#); [Rodriguez, J.](#); [Bussoletti, E.](#); [Crifo, J. F.](#); [Esposito, F.](#); [Lamy, P. L.](#); [McDonnell, J. A. M.](#); [Mennella, V.](#); [Molina, A.](#); [Morales, R.](#); [Moreno, F.](#); [Palomba, E.](#); [Perrin, J. M.](#); [Rodrigo, R.](#); [Zarnecki, J. C.](#); [Cosi, M.](#); [Giovane, F.](#); [Gustafson, B.](#); [Ortiz, J. L.](#); [Jeronimo, J. M.](#); [Leese, M. R.](#); [Herranz, M.](#); [Liuzzi, V.](#); [Lopez-Jimenez, A. C.](#)

**Publication:** Monthly Notices of the Royal Astronomical Society, Volume 462, Issue Suppl\_1, p.S210-S219 ([MNRAS Homepage](#))

**Publication Date:** 11/2016

**[4] Title:** Comet 67P/Churyumov-Gerasimenko preserved the pebbles that formed planetesimals

**Authors:** [Fulle, Marco](#); [Della Corte, V.](#); [Rotundi, A.](#); [Rietmeijer, F. J. M.](#); [Green, S. F.](#); [Weissman, P.](#); [Accolla, M.](#); [Colangeli, L.](#); [Ferrari, M.](#); [Ivanovski, S.](#); [Lopez-Moreno, J. J.](#); [Epifani, E.](#); [Mazzotta, R.](#); [Morales, R.](#); [Ortiz, J. L.](#); [Palomba, E.](#); [Palumbo, P.](#); [Rodriguez, J.](#); [Sordini, R.](#); [Zakharov, V.](#)

**Publication:** Monthly Notices of the Royal Astronomical Society, Volume 462, Issue Suppl\_1, p.S132-S137 ([MNRAS Homepage](#))

**Publication Date:** 11/2016

**[5] Title:** Evolution of the Dust Size Distribution of Comet 67P/Churyumov-Gerasimenko from 2.2 au to Perihelion

**Authors:** [Fulle, M.](#); [Marzari, F.](#); [Della Corte, V.](#); [Fornasier, S.](#); [Sierks, H.](#); [Rotundi, A.](#); [Barbieri, C.](#); [Lamy, P. L.](#); [Rodrigo, R.](#); [Koschny, D.](#); [Rickman, H.](#); [Keller, H. U.](#); [López-Moreno, J. J.](#); [Accolla, M.](#); [Agarwal, J.](#); [A'Hearn, M. F.](#); [Altobelli, N.](#); [Barucci, M. A.](#); [Bertaux, J.-L.](#); [Bertini, I.](#); [Bodewits, D.](#); [Bussoletti, E.](#); [Colangeli, L.](#); [Cosi, M.](#); [Cremonese, G.](#); [Crifo, J.-F.](#); [Da Deppo, V.](#); [Davidsson, B.](#); [Debei, S.](#); [De Cecco, M.](#); [Esposito, F.](#); [Ferrari, M.](#); [Giovane, F.](#); [Gustafson, B.](#); [Green, S. F.](#); [Groussin, O.](#); [Grün, E.](#); [Gutierrez, P.](#); [Güttler, C.](#); [Herranz, M. L.](#); [Hviid, S. F.](#); [Ip, W.](#); [Ivanovski, S. L.](#); [Jerónimo, J. M.](#); [Jorda, L.](#); [Knollenberg, J.](#); [Kramm, R.](#); [Kührt, E.](#); [Küppers, M.](#); [Lara, L.](#); [Lazzarin, M.](#); [Leese, M. R.](#); [López-Jiménez, A. C.](#); [Lucarelli, F.](#); [Mazzotta Epifani, E.](#); [McDonnell, J. A. M.](#); [Mennella, V.](#); [Molina, A.](#); [Morales, R.](#); [Moreno, F.](#); [Mottola, S.](#); [Naletto, G.](#); [Oklay, N.](#); [Ortiz, J. L.](#); [Palomba, E.](#); [Palumbo, P.](#); [Perrin, J.-M.](#); [Rietmeijer, F. J. M.](#); [Rodríguez, J.](#); [Sordini, R.](#); [Thomas, N.](#); [Tubiana, C.](#); [Vincent, J.-B.](#); [Weissman, P.](#); [Wenzel, K.-P.](#); [Zakharov, V.](#); [Zarnecki, J. C.](#)

**Publication:** The Astrophysical Journal, Volume 821, Issue 1, article id. 19, 14 pp. (2016). ([ApJ Homepage](#))

**Publication Date:** 04/2016

**[6] Title:** GIADA: shining a light on the monitoring of the comet dust production from the nucleus of 67P/Churyumov-Gerasimenko

**Authors:** [Della Corte, V.](#); [Rotundi, A.](#); [Fulle, M.](#); [Gruen, E.](#); [Weissman, P.](#); [Sordini, R.](#); [Ferrari, M.](#); [Ivanovski, S.](#); [Lucarelli, F.](#); [Accolla, M.](#); [Zakharov, V.](#); [Mazzotta Epifani, E.](#); [Lopez-Moreno, J. J.](#); [Rodriguez, J.](#); [Colangeli, L.](#)

[Palumbo, P.](#); [Bussoletti, E.](#); [Crifo, J. F.](#); [Esposito, F.](#); [Green, S. F.](#); [Lamy, P. L.](#);  
[McDonnell, J. A. M.](#); [Mennella, V.](#); [Molina, A.](#); [Morales, R.](#); [Moreno, F.](#);  
[Ortiz, J. L.](#); [Palomba, E.](#); [Perrin, J. M.](#); [Rietmeijer, F. J. M.](#); [Rodrigo, R.](#);  
[Zarnecki, J. C.](#); [Cosi, M.](#); [Giovane, F.](#); [Gustafson, B.](#); [Herranz, M. L.](#);  
[Jeronimo, J. M.](#); [Leese, M. R.](#); [Lopez-Jimenez, A. C.](#); [Altobelli, N.](#)

**Publication:** Astronomy & Astrophysics, Volume 583, id.A13, 10 pp. ([A&A Homepage](#))

**Publication** 11/2015

**Date:**

**[7] Title:** Density and Charge of Pristine Fluffy Particles from Comet 67P/Churyumov-Gerasimenko

**Authors:** [Fulle, M.](#); [Della Corte, V.](#); [Rotundi, A.](#); [Weissman, P.](#); [Juhasz, A.](#); [Szego, K.](#);  
[Sordini, R.](#); [Ferrari, M.](#); [Ivanovski, S.](#); [Lucarelli, F.](#); [Accolla, M.](#); [Merouane, S.](#);  
[Zakharov, V.](#); [Mazzotta Epifani, E.](#); [López-Moreno, J. J.](#); [Rodríguez, J.](#);  
[Colangeli, L.](#); [Palumbo, P.](#); [Grün, E.](#); [Hilchenbach, M.](#); [Bussoletti, E.](#); [Esposito, F.](#);  
[Green, S. F.](#); [Lamy, P. L.](#); [McDonnell, J. A. M.](#); [Mennella, V.](#); [Molina, A.](#);  
[Morales, R.](#); [Moreno, F.](#); [Ortiz, J. L.](#); [Palomba, E.](#); [Rodrigo, R.](#); [Zarnecki, J. C.](#);  
[Cosi, M.](#); [Giovane, F.](#); [Gustafson, B.](#); [Herranz, M. L.](#); [Jerónimo, J. M.](#);  
[Leese, M. R.](#); [López-Jiménez, A. C.](#); [Altobelli, N.](#)

**Publication:** The Astrophysical Journal Letters, Volume 802, Issue 1, article id. L12, 5 pp. (2015). ([ApJL Homepage](#))

**Publication** 03/2015

**Date:**

**[8] Title:** Dust measurements in the coma of comet 67P/Churyumov-Gerasimenko inbound to the Sun

**Authors:** [Rotundi, Alessandra](#); [Sierks, Holger](#); [Della Corte, Vincenzo](#); [Fulle, Marco](#);  
[Gutierrez, Pedro J.](#); [Lara, Luisa](#); [Barbieri, Cesare](#); [Lamy, Philippe L.](#);  
[Rodrigo, Rafael](#); [Koschny, Detlef](#); [Rickman, Hans](#); [Keller, Horst Uwe](#); [López-Moreno, José J.](#);  
[Accolla, Mario](#); [Agarwal, Jessica](#); [A'Hearn, Michael F.](#);  
[Altobelli, Nicolas](#); [Angrilli, Francesco](#); [Barucci, M. Antonietta](#); [Bertaux, Jean-Loup](#);  
[Bertini, Ivano](#); [Bodewits, Dennis](#); [Bussoletti, Ezio](#); [Colangeli, Luigi](#);  
[Cosi, Massimo](#); [Cremonese, Gabriele](#); [Crifo, Jean-Francois](#); [Da Deppo, Vania](#);  
[Davidsson, Björn](#); [Debei, Stefano](#); [De Cecco, Mariolino](#); [Esposito, Francesca](#);  
[Ferrari, Marco](#); [Fornasier, Sonia](#); [Giovane, Frank](#); [Gustafson, Bo](#); [Green, Simon F.](#);  
[Groussin, Olivier](#); [Grün, Eberhard](#); [Güttler, Carsten](#); [Herranz, Miguel L.](#);  
[Hviid, Stubbe F.](#); [Ip, Wing](#); [Ivanovski, Stavro](#); [Jerónimo, José M.](#); [Jorda, Laurent](#);  
[Knollenberg, Joerg](#); [Kramm, Rainer](#); [Kührt, Ekkehard](#); [Küppers, Michael](#);  
[Lazzarin, Monica](#); [Leese, Mark R.](#); [López-Jiménez, Antonio C.](#);  
[Lucarelli, Francesca](#); [Lowry, Stephen C.](#); [Marzari, Francesco](#);  
[Epifani, Elena](#); [Mazzotta, J. Anthony M.](#); [Mennella, Vito](#);  
[Michalik, Harald](#); [Molina, Antonio](#); [Morales, Rafael](#); [Moreno, Fernando](#);  
[Mottola, Stefano](#); [Naletto, Giampiero](#); [Oklay, Nilda](#); [Ortiz, José L.](#);  
[Palomba, Ernesto](#); [Palumbo, Pasquale](#); [Perrin, Jean-Marie](#); [Rodríguez, Julio](#);  
[Sabau, Lola](#); [Snodgrass, Colin](#); [Sordini, Roberto](#); [Thomas, Nicolas](#);  
[Tubiana, Cecilia](#); [Vincent, Jean-Baptiste](#); [Weissman, Paul](#); [Wenzel, Klaus-Peter](#);  
[Zakharov, Vladimir](#); [Zarnecki, John C.](#)

**Publication:** Science, Volume 347, Issue 6220, article id. aaa3905. ([Sci Homepage](#))

**Publication** 01/2015

**Date:**

**[9] Title:** Giada: its Status after the Rosetta Cruise Phase and On-Ground Activity in Support of the Encounter with Comet 67P/CHURYUMOV-GERASIMENKO

**Authors:** [Della Corte, V.](#); [Rotundi, A.](#); [Accolla, M.](#); [Sordini, R.](#); [Palumbo, P.](#); [Colangeli, L.](#); [Lopez-Moreno, J. J.](#); [Rodriguez, J.](#); [Rietmeijer, F. J. M.](#); [Ferrari, M.](#); [Lucarelli, F.](#); [Mazzotta Epifani, E.](#); [Ivanovski, S.](#); [Aronica, A.](#); [Cosi, M.](#); [Bussoletti, E.](#); [Crifo, J. F.](#); [Esposito, F.](#); [Fulle, M.](#); [Green, S. F.](#); [Gruen, E.](#); [Herranz, M. L.](#); [Jeronimo, J. M.](#); [Lamy, P.](#); [Lopez Jimenez, A.](#); [McDonnell, J. A. M.](#); [Mennella, V.](#); [Molina, A.](#); [Morales, R.](#); [Moreno, F.](#); [Palomba, E.](#); [Perrin, J. M.](#); [Rodrigo, R.](#); [Weissman, P.](#); [Zakharov, V.](#); [Zarnecki, J. C.](#)

**Publication:** Journal of Astronomical Instrumentation, Volume 3, Issue 1, id. 1350011-110

**Publication** 00/2014

**Date:**

**[10] Title:** Comet 67P/Churyumov-Gerasimenko: the GIADA dust environment model of the Rosetta mission target

**Authors:** [Fulle, M.](#); [Colangeli, L.](#); [Agarwal, J.](#); [Aronica, A.](#); [Della Corte, V.](#); [Esposito, F.](#); [Grün, E.](#); [Ishiguro, M.](#); [Ligustri, R.](#); [Lopez Moreno, J. J.](#); [Mazzotta Epifani, E.](#); [Milani, G.](#); [Moreno, F.](#); [Palumbo, P.](#); [Rodríguez Gómez, J.](#); [Rotundi, A.](#)

**Publication:** Astronomy and Astrophysics, Volume 522, id.A63, 17 pp. ([A&A Homepage](#))

**Publication** 11/2010

**Date:**

**Title:** The Grain Impact Analyser and Dust Accumulator (GIADA) Experiment for the Rosetta Mission: Design, Performances and First Results

**Authors:** [Colangeli, L.](#); [Lopez-Moreno, J. J.](#); [Palumbo, P.](#); [Rodriguez, J.](#); [Cosi, M.](#); [Della Corte, V.](#); [Esposito, F.](#); [Fulle, M.](#); [Herranz, M.](#); [Jeronimo, J. M.](#); [Lopez-Jimenez, A.](#); [Epifani, E.](#); [Mazzotta, E.](#); [Morales, R.](#); [Moreno, F.](#); [Palomba, E.](#); [Rotundi, A.](#)

**Publication:** Space Science Reviews, Volume 128, Issue 1-4, pp. 803-821 ([SSRv Homepage](#))

**Publication** 02/2007

**Date:**

**[11] Title:** 67P/Churyumov-Gerasimenko active areas before perihelion identified by GIADA and VIRTIS data fusion

**Authors:** Longobardo, A.; Della Corte, V.; Ivanovski, S.; Rinaldi, G.; Zakharov, V.; Rotundi, A.; Capaccioni, F.; Fulle, M.; Filacchione, G.; Palomba, E.; Palumbo, P.; Capria, M. T.; Tosi, F.; Raponi, A.; Ciarniello, M.; Bockelee-Morvan, D.; Erard, S.; Leyrat, C.; Dirri, F.

**Publication:** *Monthly Notices of the Royal Astronomical Society*, Volume 483, Issue 2, )

**Publication** 02/2019

**Date:**